Research Article

Pulmonary Circulation

Mechanical forces alter endothelin-1 signaling: comparative ovine models of congenital heart disease

Terry Zhu[1]*, Samuel Chiacchia[1]*, Rebecca J. Kameny[1], Antoni Garcia De Herreros[2], Wenhui Gong[1], Gary W. Raff[3], Jason B. Boehme[1], Emin Maltepe[1], Juan C. Lasheras[2], Stephen M. Black[4], Sanjeev A. Datar[1] and Jeffrey R. Fineman[1,5]

[1]Department of Pediatrics, University of California, San Francisco, CA, USA; [2]Institute of Engineering in Medicine, University of California, San Diego, CA, USA; [3]Department of Surgery, University of California, Davis, CA, USA; [4]Department of Medicine, University of Arizona, Tucson, AZ, USA; [5]Cardiovascular Research Institute, University of California, San Francisco, CA, USA

*These authors contributed equally.

Abstract

The risk and progression of pulmonary vascular disease in patients with congenital heart disease is dependent on the hemodynamics associated with different lesions. However, the underlying mechanisms are not understood. Endothelin-1 is a potent vasoconstrictor that plays a key role in the pathology of pulmonary vascular disease. We utilized two ovine models of congenital heart disease: (1) fetal aortopulmonary graft placement (shunt), resulting in increased flow and pressure; and (2) fetal ligation of the left pulmonary artery resulting in increased flow and normal pressure to the right lung, to investigate the hypothesis that high pressure and flow, but not flow alone, upregulates endothelin-1 signaling. Lung tissue and pulmonary arterial endothelial cells were harvested from control, shunt, and the right lung of left pulmonary artery lambs at 3–7 weeks of age. We found that lung preproendothelin-1 mRNA and protein expression were increased in shunt lambs compared to controls. Preproendothelin-1 mRNA expression was modestly increased, and protein was unchanged in left pulmonary artery lambs. These changes resulted in increased lung endothelin-1 levels in shunt lambs, while left pulmonary artery levels were similar to controls. Pulmonary arterial endothelial cells exposed to increased shear stress decreased endothelin-1 levels by five-fold, while cyclic stretch increased levels by 1.5-fold. These data suggest that pressure or an additive effect of pressure and flow, rather than increased flow alone, is the principal driver of increased endothelin signaling in congenital heart disease. Defining the molecular drivers of the pathobiology of pulmonary vascular disease due to differing mechanical forces will allow for a more targeted therapeutic approach.

Keywords

angiogenesis, apoptosis, pulmonary arterial hypertension, pulmonary endothelium, pulmonary hypertension

Date received: 27 January 2020; accepted: 1 April 2020

Pulmonary Circulation 2020; 10(2) 1–12
DOI: 10.1177/2045894020922118

Introduction

Pulmonary hypertension remains a source of significant morbidity and mortality in patients with primary or associated disease. Pulmonary arterial hypertension (PAH) is a common complication of congenital heart disease (CHD). Studies demonstrate that 4–15% of CHD patients go on to develop PAH, and PAH secondary to CHD represents over a third of pediatric PAH cases.[1–9] The associated risk of PAH is well-known to depend on the size and location of the cardiac defect. For example, patients with post-tricuspid valve lesions that expose the pulmonary vasculature to increased pulmonary blood flow (PBF) with a direct pressure stimulus from the systemic ventricle (e.g. large unrestrictive ventricular septal defects) develop pulmonary vascular disease (PVD) with a much greater incidence and

Corresponding author:
Jeffrey R. Fineman, Department of Pediatrics, University of California, San Francisco, CA, USA.
Email: jeff.fineman@ucsf.edu

severity than patients with pre-tricuspid valve defects (e.g. atrial septal defects) that result in increased PBF alone.[10–12] This difference suggests the risk of PAH depends upon the underlying mechanical forces conferred by the congenital defect, and that either elevated pulmonary pressure alone or the additive effect of both elevated pulmonary pressure and PBF rather than increased PBF alone drives the development of PVD. However, the relative contributions of pressure versus flow overload to vascular injury and the development of PVD in CHD patients remain poorly understood.

Many of the hallmark traits of PVD—including pulmonary vasoconstriction and an imbalance in cellular proliferation and apoptosis—are mediated by endothelial dysfunction and a pathologic imbalance of vasoactive substances.[13–16] The endothelin system is a well-described mediator of disease progression in PVD, contributing to vascular smooth muscle proliferation, cardiac and vascular hypertrophy, fibrosis, and inflammation, in addition to its well-known role as a singularly potent vasoconstrictor.[17–23] A wealth of evidence implicates endothelin-1 (ET-1) signaling in the pathophysiology of PVD secondary to CHD. ET-1 levels are increased in both the plasma and lung of patients with PVD and, importantly, correlate with disease prognosis.[17–23] However, specific ET-1 signaling associated with differing mechanical forces associated with CHD requires further investigation. Defining the contributions of different mechanical forces to altered molecular signaling in the vasculature will lead to more clearly defined risk factors for PVD and targeted endothelin receptor antagonist therapy according to underlying mechanism of disease.

Therefore, the objective of the current study was to discern alterations in ET-1 signaling associated with different hemodynamic states utilizing two clinically significant ovine models of CHD. Our previously established shunt model (shunt) recapitulates a large systemic-to-pulmonary communication via the in utero placement of a vascular graft between the ascending aorta and pulmonary artery (PA) of fetal lambs, resulting in postnatally increased PBF and pulmonary pressures, and many of the physiologic and morphologic characteristics of early PVD associated with CHD in humans.[24] Our recently established flow alone model (left pulmonary artery (LPA)) recapitulates a pre-tricuspid valve lesion of increased PBF without significantly increased PA pressures via fetal ligation of the LPA, resulting in isolated increased PBF to the right lung.[25] Previous RNA sequencing analysis demonstrated unique gene expression patterns between these models, and a hyperproliferative, anti-apoptotic cellular phenotype in shunt cultured primary pulmonary artery endothelial cells (PAECs).[25] To further delineate endothelin signaling in these CHD models, lung tissue from these animals was used to quantify and compare changes in expression of ET-1, preproET-1, and ECE-1. In addition, PAECs isolated from control lambs were used to measure changes in ET-1 expression due to applied fluid shear and/or pressure stresses. Having demonstrated the impact of varying hemodynamic conditions on ET-1 expression, we then sought to investigate the potential for downstream transcriptional effects of ET-1 modulation using RNA sequencing and gene set enrichment analysis.[26] These analyses revealed the effect of altered pulmonary hemodynamics on a subset of genes whose expression correlates closely to ET-1 expression and significantly enriched biological processes associated with angiogenesis and apoptosis. Finally, we probed the differential effects of ET-1 and BQ788 (a selective ET_B antagonist) on cellular angiogenesis and apoptosis. This work is the first to specifically address the role of aberrant hemodynamic derangements and altered ET-1 signaling in the pathophysiology of PVD secondary to differing hemodynamic forces associated with CHD.

Methods

Surgical preparation and animal care

For a model of increased PBF and pulse pulmonary pressure (PAP), as described previously in detail,[24] a total of five pregnant mixed-breed Western ewes (137–141 days gestation, term = 145 days) were anesthetized and an 8.0 mm Gore-tex vascular graft (~2 mm in length) was anastomosed between the main PA and ascending aorta of the fetal lamb. For a model of increased PBF without increased PAP, five late gestation pregnant ewes were anesthetized, and the LPA of the fetal lamb ligated, as described previously.[25] Control lambs were provided by either twin gestation ($n = 2$) or age-matched ($n = 3$). Four to six weeks following spontaneous delivery, control ($n = 5$), shunt ($n = 5$), or LPA ($n = 5$) lambs were anesthetized, mechanically ventilated, and instrumented for continuous hemodynamic measurement. Vital signs were monitored continuously throughout the study and animals were given intravenous fluids and prophylactic antibiotics per protocol. Harvested lung tissue was snap frozen in liquid nitrogen and stored at –80°C for future use. At the end of each study, all lambs were sacrificed by lethal injection of sodium pentobarbital followed by bilateral thoracotomy as described in the National Institutes of Health (NIH) Guidelines for the Care and Use of Laboratory Animals. All protocols and procedures were approved by the Committees on Animal Research at the University of California, San Francisco and University of California, Davis.

Isolation and culture of PA endothelial cells

Primary PA endothelial cells from control, shunt, and LPA lambs ($n = 5$ per group) were isolated from main PA, distal to the shunt anastomosis, at the bifurcation of the left and right pulmonary arteries, as described in detail previously.[27,28] Briefly, primary PAECs were isolated via the explant technique from the main PA. A segment of the

main PA was placed in a sterile dish containing Dulbecco's Modified Eagle Medium (DMEM) with appropriate supplementation. The segment was stripped of adventitia with sterile forceps and opened longitudinally, and the endothelial layer was removed by gentle rubbing with a cell scraper. Cells were grown in culture in appropriate media. After several days, moderate-sized aggregates of endothelial cells were transferred using a micropipette, grown to confluence, and then maintained in culture at 5% CO_2 at 37°C. All experiments were performed with passage-matched cells between passages 4–8.

mRNA extraction and quantitative real-time PCR

Total RNA was isolated from frozen lung tissue samples using the Direct-zol RNA Miniprep Plus kit (Zymo Research, Irvine, CA) according to the manufacturer's protocol. RNA concentration was quantified using a NanoDrop spectrophotometer (ND-1000, Thermo Fisher Scientific, Waltham, MA) and reverse transcription was performed with the RNA to cDNA EcoDry Premix (Oligo dT) (Takara Bio, Japan) using 1 μg of total RNA. Quantitative real-time PCR (qPCR) amplification was done in triplicate 20 μL reactions using PerfeCTa SYBR Green SuperMix ROX (Quantabio, Beverly, MA) on an ABI 7900HT real-time PCR System (Thermo Fisher). Gene-specific primers were designed using public PrimerQuest Tool software (Integrated DNA Technologies, Skokie, IL). qPCR results were calculated using the comparative C_T method as previously described[29] with beta-2-microglobulin as the reference gene and normalized to compare relative changes in mRNA expression in shunt and LPA ligation conditions to control.

Western blot

Proteins were extracted as previously described[27,28,30,31] and sample concentrations determined using a NanoDrop spectrophotometer (ND-1000, Thermo Fisher). Western blot was performed as described previously[27,28]; 20 μg of protein were loaded per sample and separated by 10% SDS-PAGE. Proteins were subsequently transferred to a polyvinylidene difluoride membrane (MilliporeSigma, Burlington, MA) and blocked with 5% nonfat dried milk in 130 mM NaCl and 25 mM Tris (Tris-Buffered Saline (TBS), pH 7.5) for 1 h at room temperature. Blots were incubated overnight at 4°C with primary antibodies against preproET-1, ECE-1, (Santa Cruz Biotechnology, Dallas, TX), and β-actin (Abcam, Cambridge, UK) which served as a loading control. This was followed by several washes in TBS Tween (TBST) and incubation with the species-appropriate horseradish peroxidase-conjugated secondary antibody for 1 h at 4°C. After final washes in TBST, protein bands were visualized by chemiluminescence (SuperSignal West Pico Chemiluminescent Substrate kit, Thermo Fisher). Relative protein expression was calculated by band densitometry using the public domain Java image-processing program ImageJ (NIH Image).

Endothelin Converting Enzyme (ECE) activity

ECE activity was measured with the SensoLyte 520 ECEs Activity Assay Kit Fluorimetric (AnaSpec, Fremont, CA). Cells were collected and lysed at density of ~5e5 cells/mL; 50 μL of lysates were used to run assay per manufacturer protocol; and 0.2 ng/μL of human, recombinant ECE-1 (AnaSpec, Fremont, CA) was used as positive control. Reference standards were generated according to manufacturer instructions. Assay plate was incubated for 30 min at 37°C. Endpoint readings were measured in relative fluorescence units (RFUs) at Ex/Em 490 nm/520 nm using spectrophotometer.

ET-1 determinations

Proteins were extracted from lung tissue by homogenization in radioimmunoprecipitation (RIPA) buffer (150 mM NaCl, 1% Nonidet P-40, 0.25% sodium deoxycholate, 1 mM EDTA, 50 mM Tris-HCl) containing a protease inhibitor cocktail (Sigma Aldrich, St. Louis, MO) followed by sonification and centrifugation to collect liquid lysate. Whole cell lysates were similarly extracted from PAECs by scraping and sonicating cells in RIPA buffer with protease inhibitors (Sigma Aldrich). Protein concentrations were then determined for lung homogenates via a Bicinchoninic Acid Protein Assay Kit (Sigma Aldrich) and for whole cell lysates via Quick Start Bradford Protein Assay (Bio-Rad, Hercules, CA). ET-1 ELISA was performed using a commercial kit according to the manufacturer's instructions (Enzo Life Sciences, Farmingdale, NY), as we have previously described.[30–32] The sensitivity is 0.41 pg/mL with a range of 0.78–100 pg/mL. Standard and sample concentrations were calculated by fitting the data to a four-parameter logistic regression.

Fluid shear stress and cyclical stretch stress

For fluid shear stress, cells were maintained in DMEM containing 1% serum and 10 μg/mL heparin on six-well tissue culture plates (Costar) for 24 h before initiating shear stress experiments. A cone-plate viscometer was designed and built such that it accepts six-well plates.[27,28] This allowed the PAEC monolayer to be subjected to a radially constant fluid shear stress at laminar flow rates representing levels of shear stress within physiologic parameters. Typical physiologic shear stress in the major human arteries is in the range of 5–20 dynes/cm^2.[33] Thus, we imparted a shear stress of 20 dynes/cm^2 for 8 h to mimic the upper limit of the physiologic range. For cyclic stretch, cells were maintained in DMEM containing 1% serum and 10 μg/mL heparin on six-well

BioFlex plates coated with collagen type I (FlexCell) for 24 h, then subjected to biaxial cyclic stretch using the FlexCell 3000 Strain Unit. Plates were placed on a loading station and stretched by applying an oscillatory vacuum to the underside of the membranes. Cells were stretched at a frequency of 1 Hz with 20% amplitude for 8 h in accordance with previous studies.[34]

RNA sequencing analysis

Previous RNA sequencing analysis demonstrated that *EDN1* (ET-1) was a top 10 up-regulated transcript in shunt compared to LPA and control PAECs.[25] To determine the potential impact of *EDN1* on the angiogenic, anti-apoptotic phenotype of these shunt PAECs, IPA Pathway Analysis (Qiagen, Inc) was utilized to generate networks of differentially expressed genes (DEGs) (False Discovery Rate (FDR) <0.05; FE >2) downstream of *EDN1*. In addition, we searched our database of DEGs for transcripts that adhere to *EDN1's* unique expression pattern (i.e. elevated in shunt, depressed in LPA). Of the 1069 genes that were significantly elevated in shunt PAECs, 136 (13%) were also significantly depressed in PAECs from LPA animals. To gain a more complete understanding of how these unique DEGs may influence biology, they were submitted to the Gene Ontology (GO) database for pathway enrichment analysis. Source material was RNA obtained from PAEC clonal lines derived from control ($n=4$), LPA ($n=3$), or shunt ($n=2$) lambs.

Angiogenesis quantification

Matrigel assays were performed in 24-well plates previously coated with 50 μL/cm^2 of Corning Matrigel Basement Membrane Matrix (Corning #354234; 9 mg/mL, Tewksbury, MA, USA) as previously described.[25] Cells were seeded (40,000 cells/well, passage 2–5) and adhered for 4–6 h. After 72 h, four pictures/well were taken using the Cell Imaging System EVOS, and automatic quantification of tube formation was performed with the Image J Angiogenesis Analyzer. Briefly, the length was calculated in order to quantify the capacity of PAECs for tube formation. Comparisons were made between baseline conditions and with the addition of either ET-1 (1 μM/mL) or BQ788 (an ET_B receptor antagonist, 1 μM/mL).

Apoptosis quantification

Terminal deoxynucleotidyl transferase 2'-deoxyuridine 5'-triphosphate (dUTP) nick end labeling analysis. Terminal deoxynucleotidyl transferase dUTP nick end labeling (TUNEL) assay was performed using the DeadEnd Colorimetric Apoptosis Detection System (Promega) as previously described.[35,36] Briefly, PAECs from each experimental group (control, LPA, and shunt) were treated with tumor necrosis factor (TNF)-α 50 ng/mL. After TNF-α treatment, cells were appropriately washed and fixed, then incubated with terminal deoxynucleotidyl transferase and reaction mix including fluorescein-12-dUTP for 1 h at 37°C. Cells were then again washed and incubated with 4′,6-diamidino-2-phenylindole (DAPI) (5 μM) for 15 min at room temperature. DAPI, a nuclear stain, was used normalize for total cell number. Comparisons were made between baseline conditions and with the addition of either ET-1 (1 μM/mL) or BQ788 (an ET_B receptor antagonist, 1 μM/mL).

Statistical analysis

Data are represented as mean ± SD. Statistical significance was determined by one-way analysis of variance with post-hoc Tukey's tests. A p-value <0.05 was taken to be statistically significant.

Results

We previously demonstrated the hemodynamic differences in the lamb models.[25] As expected, both LPA ligation and shunt lambs had significantly higher right PBF, compared to controls, while shunt lambs had higher mean PA pressure compared to both control and LPA lambs[25] (Table 1).

Peripheral lung preproET-1 mRNA expression was increased in shunt lambs compared to both control and LPA ligation lambs (Fig. 1a). Compared to controls, preproET-1 mRNA expression was modestly increased in LPA lambs (Fig. 1a). ECE-1 mRNA expression was similarly increased in shunt and LPA lambs compared to controls (Fig. 1b). Lung preproET-1 and ECE-1 protein levels were increased in shunt lambs compared to both control and LPA ligation lambs (Fig. 1c and d). Compared to controls, both preproET-1 and ECE-1 protein levels were modestly increased in LPA lambs (Fig. 1d). ECE-1 activity was similar in all three groups (744.1 ± 21.8 RFU control; 724.6 ± 54.6 RFU shunt; 731.2 ± 68.7 RFU LPA, $n=3$ in each group). These changes resulted in increased lung ET-1

Table 1. Baseline hemodynamics in Control ($n=9$), LPA ligation ($n=8$), shunt ($n=4$) lambs.

	MAP (mmHg)	MPAP (mmHg)	Δ PAP (mmHg)	RPAQ (L/min)
Control	70 ± 9.4	14 ± 1.8	11.8 ± 0.2	0.7 ± 0.1
LPA	74 ± 15	19 ± 3.6[a]	14.8 ± 3.2	1.4 ± 0.3[a]
Shunt	61 ± 8.7	26 ± 6.3[a,b]	18 ± 0.4[a,b]	2.0 ± 0.2[a,b]

[a] $p < 0.05$ vs control.

[b] $p < 0.05$ shunt vs LPA ligation lambs.

Notes: In order to compare pulmonary blood flow between the three groups, right pulmonary artery blood flow (RPAQ) was estimated assuming 55% of total pulmonary blood flow, for control and shunt lambs.

MAP: mean arterial pressure; MPAP: mean pulmonary arterial pressure; ΔPAP: pulse pulmonary pressure; RPAQ: right lung pulmonary artery blood flow.

Source: reproduced with permission from Johnson Kameny et al., 2019.[25]

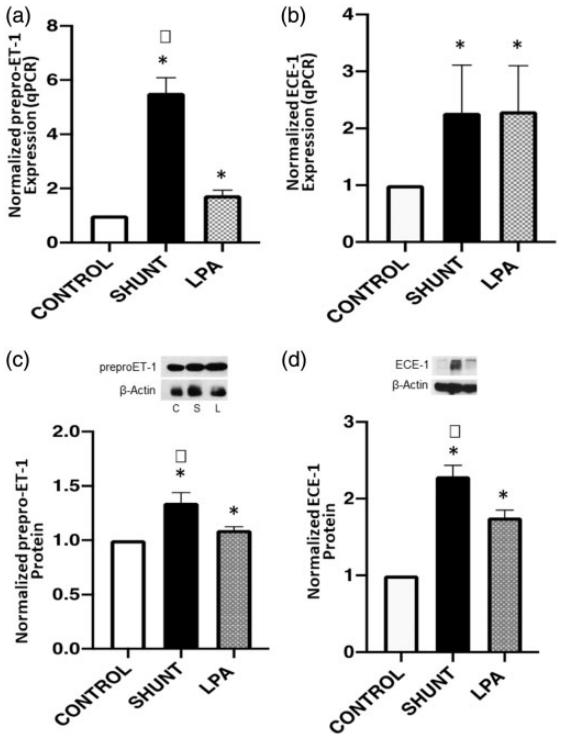

Fig. 1. Lung preproET-1 mRNA and protein expression were increased in shunt lambs compared to controls (a and c) ($p < 0.05$). PreproET-1 mRNA expression was unchanged in LPA lambs, and protein was modestly increased (a and c). In both shunt and LPA lambs, ECE-1 mRNA and protein expression were increased compared to controls (b and d) ($p < 0.05$). In addition, shunt ECE-1 mRNA and protein expression were increased compared to LPA (b and d). Representative images of western blots (c and d) are shown. In all panels, shunt and LPA values are normalized to control. Values are mean ± SD, $n = 5$ for each group, *vs. control; †vs. LPA $p < 0.05$.
LPA: left pulmonary artery; ET-1: endothelin-1; qPCR: quantitative real-time PCR.

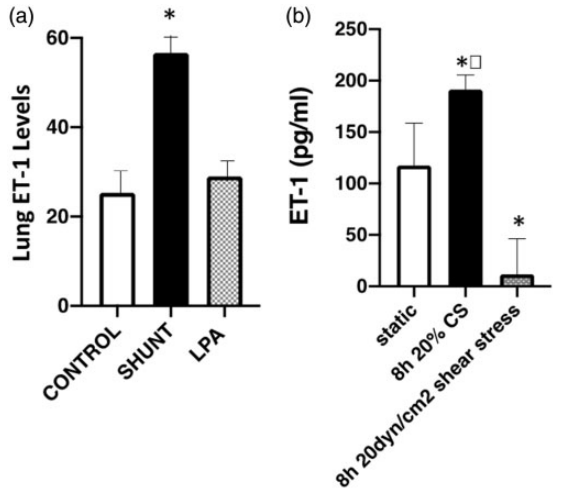

Fig. 2. Peripheral lung tissue levels of ET-1 (ELISA) are increased in shunt lambs, but not LPA lambs (a). $n = 5$ for each group, * vs. control $p < 0.05$. Control PAECs exposed to 8 h of shear stress (20 dyn/cm^2) decreases ET-1 levels; 8 h of cyclic stretch (CS, 20%) increases ET-1 levels (b). $n = 5$, *vs. static; †vs. LPA $p < 0.05$.
LPA: left pulmonary artery; ET-1: endothelin-1.

levels in shunt lambs, while LPA levels were similar to controls (Fig. 2a). Interestingly, the application of cyclic stretch to control PAECs increased ET-1 levels, while the application of fluid shear stress decreased ET-1 levels (Fig. 2b).

Importantly, previous RNAseq evaluation on PAECs harvested from the main PA from each model demonstrated ET-1 (*EDN1*) as a top upregulated gene in shunt lambs that was uniquely downregulated in LPA ligation lambs compared to controls.[25] Dendrogram and unsupervised hierarchical clustering heat map analysis demonstrate excellent differentiation between PAECs derived from each model (Fig. 3).

Given the relationship between ET-1 expression and hemodynamics in the pulmonary vasculature, we hypothesized that downstream changes in gene transcription related to ET-1 would be observed in PAECs and these changes might shed light on the pathophysiology of PVD. We utilized RNAseq data derived from PAECs taken from shunt, LPA, and control animals to investigate changes in gene expression associated with ET-1. After generating a list of significantly DEGs (FDR <0.05, FE > 2), we then used IPA Pathway Analysis (Qiagen, Inc) to produce a set of likely transcription networks downstream of *EDN1*. DEGs shown in orange are predicted to be activated, while those in blue are predicted to be inhibited (Fig. 4a and c). We then utilized IPA knowledge database to highlight terms associated with either angiogenesis or apoptosis as indicated by light blue dashed lines. These results suggest that ET-1 likely exerts additional downstream effects on PAEC pathology through direct transcriptional regulation of genes related to angiogenesis and apoptosis.

Additionally, we hypothesized that changes in ET-1 expression could have indirect influence on gene expression given its function as a potent vasoconstrictor. To test this hypothesis, we identified a subset of genes with expression patterns correlated to ET-1 expression (i.e. elevated in shunt PAEC and depressed in LPA PAEC). Of the 1069 genes that were significantly elevated in shunt PAECs, 136 (13%) were also significantly depressed in PAECs from LPA animals with respect to control. To gain a more complete understanding of how these DEGs may influence PAEC biology, they were submitted to the GO database for pathway enrichment analysis. Doing so revealed a total of 152 significantly enriched biological processes (FDR <0.05; FE > 2). Among the most significant pathways included associated angiogenesis (GO:0001525) (Fig. 4a and b) and negative regulation of apoptosis (GO:0043066) (Fig. 4c and d).

To more directly determine a potential role for the differential *EDN1* in relation to the angiogenic, anti-apoptotic shunt cellular phenotype, we determined the effect of ET-1

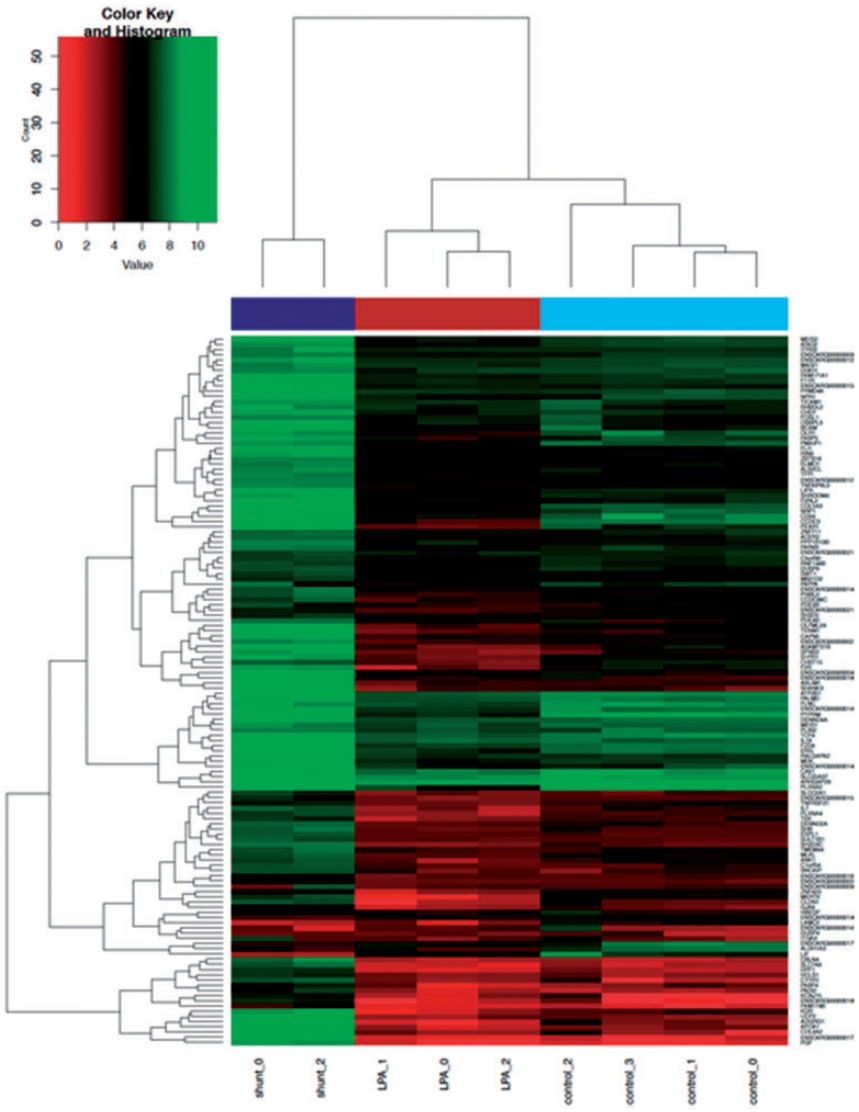

Fig. 3. *EDN1* transcriptional characterization of control, LPA and shunt PAECs. $n = 4$ control, $n = 3$ LPA, $n = 2$ shunt. Gene expression of the 136 significant DEGs exhibiting expression patterns similar to *EDN1* with respect to animal model hemodynamics (q-value <0.05) are represented here in a heatmap. Expression is quantified by log fragments per kilobase million (FPKM) where green indicates relatively higher levels of expression and red represents lower levels. Heat map of PAEC RNA-Seq data confirm clustering of gene expression by model.
LPA: left pulmonary artery.

and ET_B receptor blockade on: (1) tube formation length in growth factor restricted Matrigel to characterize angiogenesis and (2) TUNEL staining following TNF-α stimulation to induce apoptosis. As seen in Fig. 5a and b, at baseline, PAECs from shunt animals had a greater rate of angiogenesis compared to control and LPA cells after 72 h in Matrigel, as quantified by increased tube formation length. The addition of ET-1 had no effect on control or shunt cells, but increased LPA tube length to that of shunt PAECs, suggesting a primed LPA phenotype. ET_B receptor blockade decreased shunt tube length to control values. As seen in Fig. 6a and b, control PAECs had the greatest percentage of apoptotic cells, followed by LPA PAECs, with shunt PAECs exhibiting the greatest resistance to apoptosis (Fig. 6a and b). The addition of ET-1 decreased apoptosis in control, LPA, and shunt cells. ET_B receptor blockade did not alter apoptosis rates in control or LPA cells, but increased shunt cells above its respective baseline values.

Discussion

PVD is associated with a spectrum of pathology that includes chronic hypoxic conditions, infections, chronic inflammatory states, drug/toxin-induced, and genetic etiologies.[1] Although the late symptoms and histopathology of these differing etiologies are similar, their initial

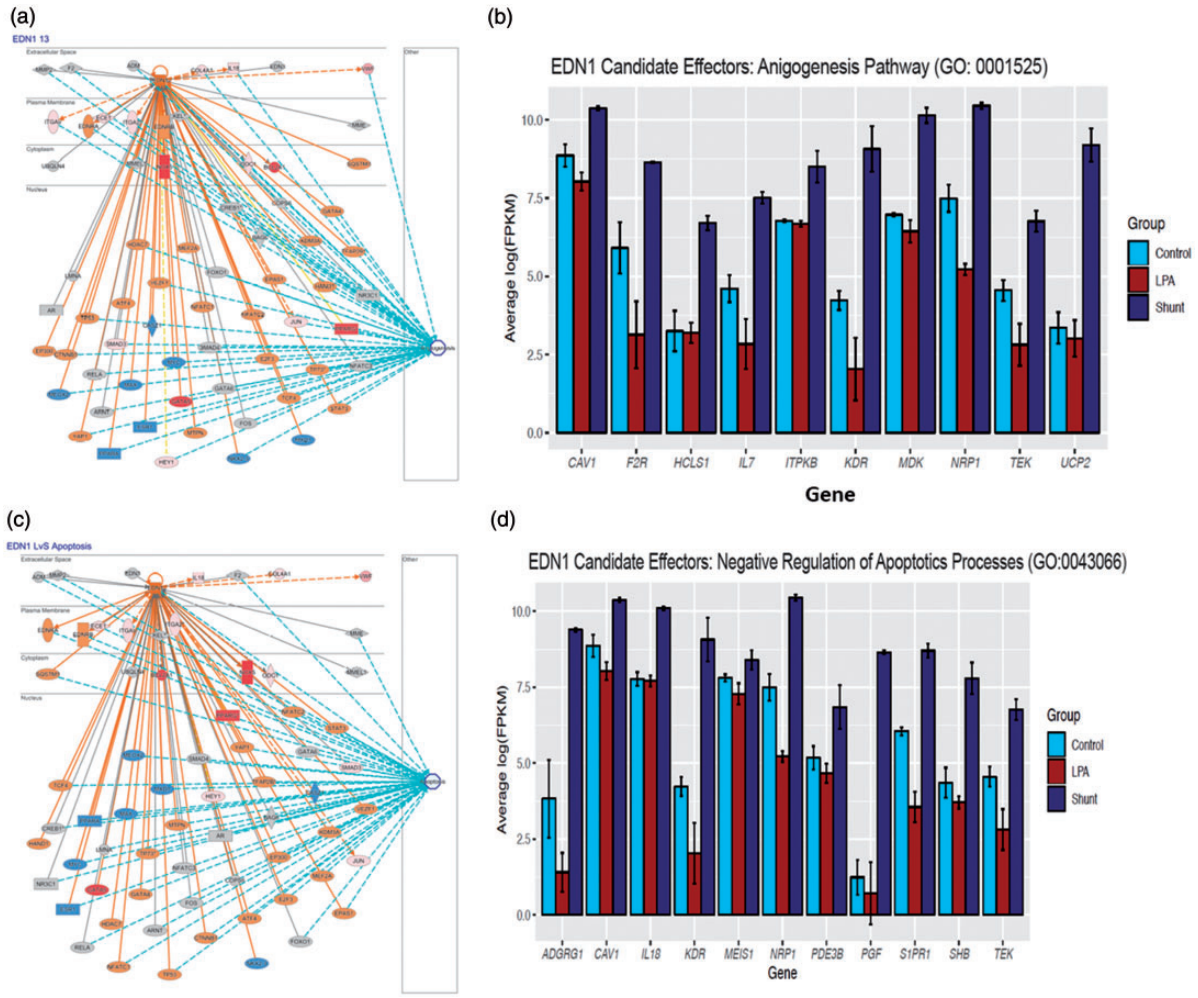

Fig. 4. IPA Pathway Analysis (Qiagen, Inc) was utilized to generate networks of differentially expressed genes (DEG) (FDR <0.05; FE >2) downstream of *EDN1* (a and c). DEGs shown in orange are predicted to be activated, while those in blue are predicted to be inhibited. We then utilized IPA knowledge database to highlight terms associated with either angiogenesis or apoptosis as indicated by light blue dashed lines. We searched our PAEC dataset of differentially expressed genes for transcripts that adhere to *EDN1*'s unique expression pattern (i.e. elevated in shunt, depressed in LPA). These unique 136 DEGs were submitted to the Gene Ontology (GO) database for pathway enrichment analysis which revealed a total of 152 significantly enriched biological processes (FDR <0.05; fold enrichment (FE) >2). Among the most significant pathways associated with PVD physiology, were associated angiogenesis (b) and negative regulation of apoptotic process (d). For each pathway, mean expressions of candidate effector genes are displayed.
LPA: left pulmonary artery.

pathobiology is likely disparate. CHD-associated PVD is a common pediatric etiology of PVD, but unique in several aspects: (1) the inciting event, or trigger, is known (exposure of the pulmonary vasculature to abnormal mechanical forces); (2) there is an understanding of the natural history of disease progression, and an insight into early disease; (3) persistence of the abnormal forces leads to progressive PVD that shares many characteristics with other forms of PVD; (4) timely removal of these forces with surgical correction results in complete disease reversal; and (5) the subgroup of patients that do not reverse PVD despite surgical correction facilitates the potential identification of conditions and mechanisms specifically associated with (the transition towards) irreversible disease.[37] In the current study, we utilized two differing ovine models of CHD to determine potential differences in ET-1 expression associated with different forms of CHD. In fact, we found that ET-1 expression was preferentially increased in our shunt model as compared to our LPA ligation model. Our shunt model mimics cardiac defects that are most at risk for developing irreversible PVD without early surgical repair, cardiac defects that induce increased PBF plus a direct pressure stimulus from the systemic ventricle on the pulmonary circulation (e.g. non-restrictive VSD).[24] Our LPA ligation model mimics cardiac defects (e.g. Atrial Septal Defects (ASD)) that have a much lower incidence of developing PVD, pre-tricuspid valve defects that induce increased PBF alone.[25] These findings were recapitulated in vitro, in

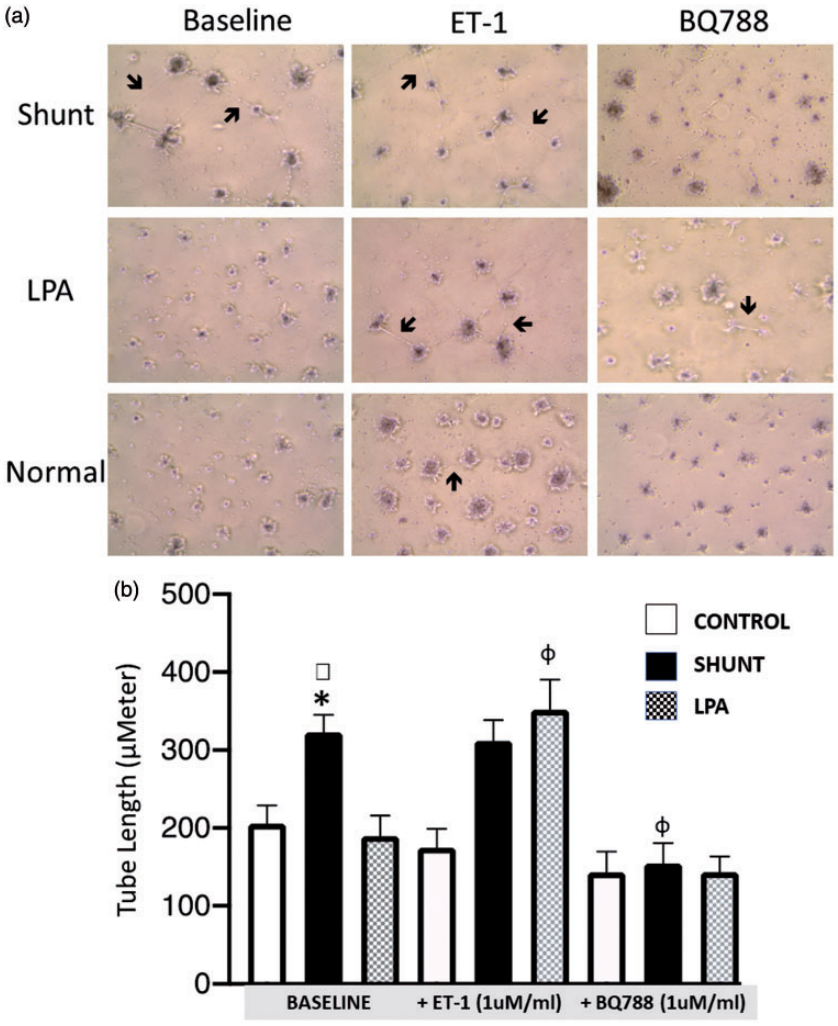

Fig. 5. PAECs angiogenic capacity was assess using Matrigel assay. Over a 72-h period, both shunt PAECs formed tubes of longer length that PAECs isolated from control lambs, while shunt PAECs from LPA animals had a similar tube length to controls. The addition of ET-1 (1 μM/mL) increased tube length in cells harvested from LPA lambs, but did not change tube length in cells harvested from control or shunt lambs. The addition of BQ788 (1 μM/mL, an ET_B receptor antagonist) decreased tube length in shunt PAECs but did not change tube length in control or LPA PAECs. $n = 5$ per group. (a) representative photos; (b) quantification. *$p < 0.05$ vs. baseline controls; †$p < 0.05$ vs. baseline LPA; $\varphi p < 0.05$ vs. corresponding baseline cell model.
LPA: left pulmonary artery; ET-1: endothelin-1.

which cyclic stretch, the mechanical force associated with increased pressure, increased ET-1 signaling, while increased shear stress, the mechanical force associated with increased flow, decreased ET-1 signaling.

Taken together, this study provides both in vivo and in vitro evidence that pressure (stretch) is the major driver of ET-1 upregulation. The effects of ET-1 gene expression and release have been previously studied with diverse in vitro study designs.[38–45] These studies demonstrate varying results, but they differed by the cell type studied, and the type, extent, and duration of the mechanical force utilized. For example, studies in human umbilical venous endothelial cells consistently demonstrate a decrease in ET-1 release, preproET-1, and ECE-1 expression in response to increased shear stress.[38,39,42,43] However, cyclic stretch increases preproET-1 expression but systemic levels of pressure decrease ET-1 release.[38–40] Studies in systemic vascular ECs consistently demonstrate an increase in ET-1 release and preproET-1 expression in response to cyclic stretch or systemic levels of pressure.[41,44] Similar to our study, the only previous study in PAECs demonstrated a decrease in ET-1 release with an increase in shear stress from 5 dyn/cm^2 to 20 dyn/cm^2. However, further increases to pathologic levels of shear stress (120 dyn/cm^2) increased ET-1.[45] The current study is the first to evaluate differing mechanical forces by comparing both in vivo models and in vitro forces. Interestingly, RNAseq analysis from cells cultured from our animal models correlates exactly with our in vitro studies; PAECs isolated from shunt lambs exposed to increased pressure in vivo and PAECs isolated from normal lambs exposed

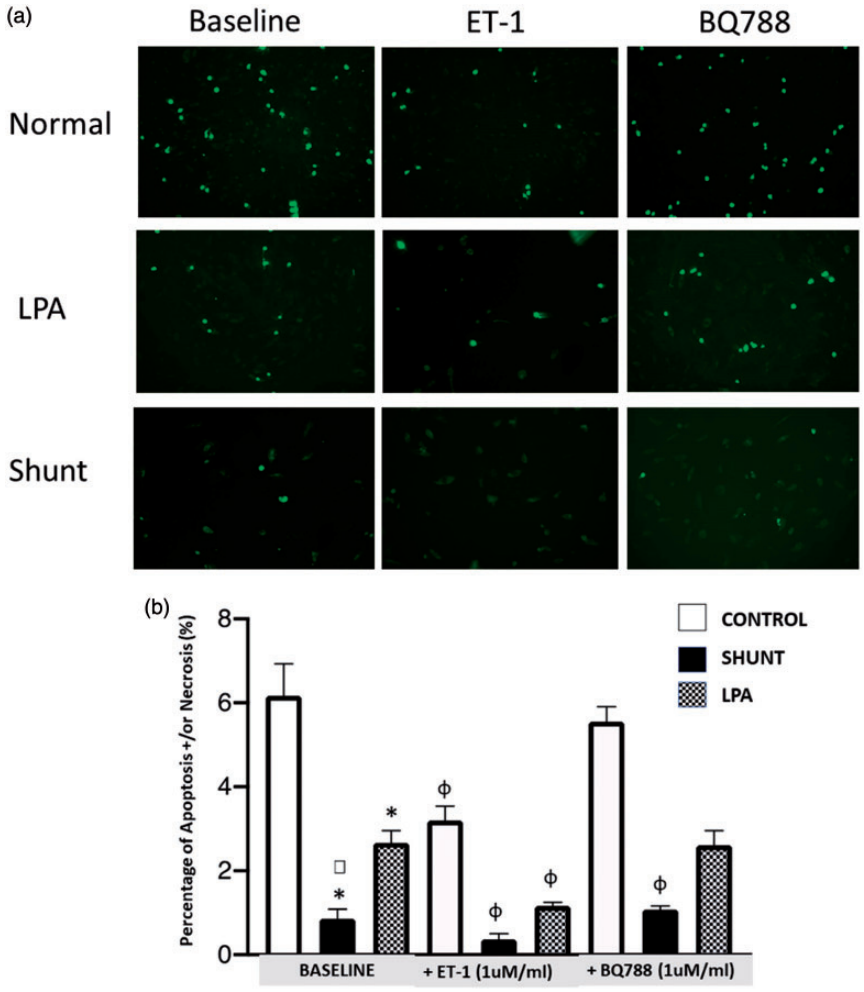

Fig. 6. PAECs apoptosis susceptibility was assessed using TUNEL assay following TNF-α treatment to induce apoptosis. Over a 24-h period, both LPA and shunt PAECs had less apoptosis than did PAECs isolated from control lambs, while shunt PAECs had even less apoptosis than did PAECs derived from LPA lambs. The addition of ET-1 (1 μM/mL) decreased apoptosis in cells from each animal model. The addition of BQ788 (1 μM/mL, an ET_B receptor antagonist) increased apoptosis in shunt PAECs. $n = 5$ per group. (a) representative photos; (b) quantification.
*$p < 0.05$ vs. baseline controls; †$p < 0.05$ vs. baseline LPA; $\varphi p < 0.05$ vs. corresponding baseline cell model.
LPA: left pulmonary artery; ET-1: endothelin-1.

to cyclic stretch in vitro both increased ET-1 RNA expression, while PAECs isolated from LPA ligation lambs exposed to increased flow alone in vivo and PAECs isolated from normal lambs exposed to shear stress in vitro both decreased RNA ET-1 expression (Fig. 2). However, studies from peripheral lung correlate less precisely suggesting that the differing cell types in lung homogenate likely alter the results slightly. For example, in peripheral lung from shunt lambs, ET-1, ECE-1, and ET production were increased compared to both LPA and control lambs, correlating with the increased ET-1 levels in shunt lambs. However, despite the fact that ET-1 levels in peripheral lung from LPA lambs was similar to controls, ET-1 and ECE-1 expression was modestly increased in peripheral lung from LPA ligation lambs compared to controls (Figs 1 and 2).

Our previous study demonstrated an increase in the number of pulmonary vascular arterioles in shunt compared to control four-week-old lambs.[24] This doubling of pulmonary vessels may represent an early compensatory angiogenesis to incorporate the increased flow and pressure. Importantly, this angiogenesis is not appreciated in our flow alone LPA ligation lambs (unpublished observation). In addition, we recently demonstrated a hyperproliferative, angiogenic, anti-apoptotic phenotype in cells harvested from shunt PA, but not in LPA cells.[25] To determine a potential role for ET-1 in this phenotype, we utilized IPA Knowledge and GO databases that revealed significantly enriched biological pathways that included angiogenesis and negative regulation of apoptosis, suggesting that ET-1 activity may influence the expression of other genes whose functions relate to this phenotype (Fig. 4). In addition, as seen in Figs 5 and 6, in vitro assays demonstrate that the addition of ET-1 or the ET_B receptor antagonist BQ788 directly influences these functions. Further studies are warranted

to determine if this early EC phenotype of hyperproliferation, angiogenetic, and anti-apoptotic is initially an adaptive response to incorporate the increase in flow and pressure that with increasing time will contribute to the pathologic remodeling associated with the development of PVD.

Although these data clearly demonstrate that increased pressure in vivo, and cyclic stretch in vitro, upregulate ET-1 expression, a significant limitation of the current study is that the mechanism by which the mechanotransduction of pressure or stretch upregulates ET-1 is not investigated. We are currently evaluating several potential mechanisms that include alterations in reactive oxygen species (ROS) and hypoxia-inducible factors (HIF)-1 and -2. For example, data suggest that cyclic stretch increases mitochondrial ROS production, which can stimulate HIF-1α activity, and the induction of several HIF-1α-dependent genes including ET-1 expression.[46–48] We have previously demonstrated increases in ROS in shunt lambs, and this ROS/HIF-1/ET-1 pathway has been implicated in the cardiovascular complications of obstructive sleep apnea.[49,50] This potential mechanism in CHD requires further investigation and is beyond the scope of this manuscript.

This is the first investigation of the differential effects of in vivo and in vitro mechanical forces associated with different types of CHD on ET-1. Our results suggest that pressure-driven lesions that are associated with cyclic stretch and a greater risk of developing PVD are associated with an upregulation of ET-1 signaling and production. In addition, directly and/or indirectly, ET-1 signaling may be related to the cellular hyperproliferative phenotype demonstrated in shunt PAECs. The development of new therapies over the past decade has certainly improved outcomes of patients with PVD. However, morbidity and mortality remain unacceptably high, and our current therapeutic approach remains suboptimal on several fronts that include: (1) currently only three signaling cascades are targeted (Nitric oxide-cGMP, prostacyclin, ET-1) and (2) the treatment approach is similar in all forms of PVD despite the differential pathobiology, and relates to disease severity as opposed to underlying pathology.[51] In this study, we focus on one form on PVD, that associated with CHD, and evaluate differential signaling of one of the current therapeutic targets, ET-1. We speculate that further translational investigations that discern particular aberrations in PH biology within subsets of patients could facilitate a more tailored therapeutic approach for clinicians within different types of PVD. For example, our results would suggest that a PVD treatment prevention strategy in a patient with CHD whose surgery requires delay, may be dependent upon their underlying physiology; a treatment strategy in a patient with CHD associated with increased PBF alone may not include an ET receptor antagonist, while a patient with CHD resulting in both increased flow and a direct pressure stimulus may include an ET receptor antagonist. Further studies are warranted to better inform these types of therapeutic decisions.

Acknowledgments

The authors would like to thank Rachel Hutchings, Linda Talkin, Courtney Losser, and Christian Vento for their expert technical support.

Author contributions

T.Z., R.J.K., S.A.D., and J.R.F. conceived and designed research; S.C. performed the RNA sequencing analysis; A.G.H., J.C. L., and S.M.B. performed the mechanical forces studies; S.M.B. prepared figures; W.G., E.M., and J.B.B. performed the biochemical studies; G.W.R., R.J.K., S.A.D., and J.B.B. performed the animal surgery. All authors edited, revised manuscript, and approved final version of the manuscript.

Conflict of interest

The author(s) declare that there is no conflict of interest.

Funding

This research was supported by grants from the National Institutes of Health (HL61284 and HL137282 to J.R.F., 5T32HD049303-07 to J.R.F. and R.J.K., HD072455 to E.M., HL133034 to S.A.D., and K08HL146933 to R.J.K.) and American Heart Association (14FTF19670001 to R.J.K.).

Guarantor

Jeffrey R. Fineman

References

1. Simonneau G, Robbins IM, Beghetti M, et al. Updated clinical classification of pulmonary hypertension. *J Am Coll Cardiol* 2009; 54: S43–S54.
2. Haworth SG and Hislop AA. Treatment and survival in children with pulmonary arterial hypertension: the UK Pulmonary Hypertension Service for Children 2001–2006. *Heart* 2009; 95: 312–317.
3. Hoffman JI, Rudolph AM and Heymann MA. Pulmonary vascular disease with congenital heart lesions: pathologic features and causes. *Circulation* 1981; 64: 873–877.
4. Kouchoukos NT, Blackstone EH and Kirklin JW. Surgical implications of pulmonary hypertension in congenital heart disease. *Adv Cardiol* 1978; 22: 225–231.
5. Adatia I, Kothari SS and Feinstein JA. Pulmonary hypertension associated with congenital heart disease: pulmonary vascular disease: the global perspective. *Chest* 2010; 137: 52S–61S.
6. Butrous G, Ghofrani HA and Grimminger F. Pulmonary vascular disease in the developing world. *Circulation* 2008; 118: 1758–1766.
7. Duffels MG, Engelfriet PM, Berger RM, et al. Pulmonary arterial hypertension in congenital heart disease: an epidemiologic perspective from a Dutch registry. *Int J Cardiol* 2007; 120: 198–204.
8. Manes A, Palazzini M, Leci E, et al. Current era survival of patients with pulmonary arterial hypertension associated with congenital heart disease: a comparison between clinical subgroups. *Eur Heart J* 2014; 35: 716–724.
9. Berger RM, Beghetti M, Humpl T, et al. Clinical features of paediatric pulmonary hypertension: a registry study. *Lancet* 2012; 379: 537–546.

10. Hoffman JI and Rudolph AM. The natural history of ventricular septal defects in infancy. *Am J Cardiol* 1965; 16: 634–653.
11. Hoffman JI, Rudolph AM and Danilowicz D. Left to right atrial shunts in infants. *Am J Cardiol* 1972; 30: 868–875.
12. Hallidie-Smith KA, Hollman A, Cleland WP, et al. Effects of surgical closure of ventricular septal defects upon pulmonary vascular disease. *Br Heart J* 1969; 31: 246–260.
13. Rabinovitch M, Bothwell T, Hayakawa BN, et al. Pulmonary artery endothelial abnormalities in patients with congenital heart defects and pulmonary hypertension. A correlation of light with scanning electron microscopy and transmission electron microscopy. *Lab Invest* 1986; 55: 632–653.
14. Rabinovitch M. Molecular pathogenesis of pulmonary arterial hypertension. *J Clin Invest* 2008; 118: 2372–2379.
15. Budhiraja R, Tuder RM and Hassoun PM. Endothelial dysfunction in pulmonary hypertension. *Circulation* 2004; 109: 159.
16. Adatia I, Barrow SE, Stratton PD, et al. Thromboxane A2 and prostacyclin biosynthesis in children and adolescents with pulmonary vascular disease. *Circulation* 1993; 88: 2117–2122.
17. Chester AH and Yacoub MH. The role of endothelin-1 in pulmonary arterial hypertension. *Glob Cardiol Sci Pract* 2014; 2014: 62–78.
18. Dhuan N and Webb DJ. Endothelins in cardiovascular biology and therapeutics. *Nat Rev Cardiol* 2019; 16: 491–502.
19. Beghetti M, Black SM and Fineman JR. Endothelin-1 in congenital heart disease. *Pediatr Res* 2005; 57: 16R.
20. GaliÃ© N, Manes A and Branzi A. The endothelin system in pulmonary arterial hypertension. *Cardiovasc Res* 2004; 61: 227–237.
21. Giaid A, Yanagisawa M, Langleben D, et al. Expression of endothelin-1 in the lungs of patients with pulmonary hypertension. *N Engl J Med* 1993; 328: 1732–1739.
22. Yoshibayashi M, Nishioka K, Nakao K, et al. Plasma endothelin concentrations in patients with pulmonary hypertension associated with congenital heart defects. Evidence for increased production of endothelin in pulmonary circulation. *Circulation* 1991; 84: 2280–2285.
23. Komai H, Adatia IT, Elliott MJ, et al. Increased plasma levels of endothelin-1 after cardiopulmonary bypass in patients with pulmonary hypertension and congenital heart disease. *J Thorac Cardiovasc Surg* 1993; 106: 473–478.
24. Reddy VM, Meyrick B, Wong J, et al. In utero placement of aortopulmonary shunts. A model of postnatal pulmonary hypertension with increased pulmonary blood flow in lambs. *Circulation* 1995; 92: 606–613.
25. Johnson Kameny R, Datar SA, Boehme JB, et al. Ovine models of congenital heart disease and the consequences of hemodynamic alterations for pulmonary artery remodeling. *Am J Respir Cell Mol Biol* 2019; 60: 503–514.
26. Hänzelmann S, Castelo R and Guinney J. GSVA: gene set variation analysis for microarray and RNA-seq data. *BMC Bioinformatics* 2013; 14: 7.
27. Wedgwood S, Mitchell CJ, Fineman JR, et al. Developmental differences in the shear stress-induced expression of endothelial NO synthase: changing role of AP-1. *Am J Physiol Lung Cell Mol Physiol* 2003; 284: L650–L662.
28. Wedgwood S, Bekker JM and Black SM. Shear stress regulation of endothelial NOS in fetal pulmonary arterial endothelial cells involves PKC. *Am J Physiol Lung Cell Mol Physiol* 2001; 281: L498.
29. Schmittgen TD and Livak KJ. Analyzing real-time PCR data by the comparative CT method. *Nat Protoc* 2008; 3: 1101.
30. Black SM, Bekker JM, Johengen MJ, et al. Altered regulation of the ET-1 cascade in lambs with increased pulmonary blood flow and pulmonary hypertension. *Pediatr Res* 2000; 47: 97–106.
31. McMullan MD, Bekker JM, Johengen MJ, et al. Inhaled nitric oxide-induced rebound pulmonary hypertension: role for endothelin-1. *Am J Physiol Heart Circ Physiol* 2001; 280: H785.
32. Wong J, Reddy VM, Hendricks-Munoz K, et al. Endothelin-1 vasoactive responses in lambs with pulmonary hypertension and increased pulmonary blood flow. *Am J Physiol* 1995; 269: H1965–H1972.
33. Dewey CF Jr, Bussolari SR, Gimbrone MA Jr, et al. The dynamic response of vascular endothelial cells to fluid shear stress. *J Biomech Eng* 1981; 103: 177–185.
34. Quinn TP, Schlueter M, Soifer SJ, et al. Cyclic mechanical stretch induces VEGF and FGF-2 expression in pulmonary vascular smooth muscle cells. *Am J Physiol Lung Cell Mol Physiol* 2002; 282: L897–L903.
35. Cohen JJ, Duke RC, Fadok VA, et al. Apoptosis and programmed cell death in immunity. *Annu Rev Immunol* 1992; 10: 267–293.
36. Wedgwood S and Black SM. Molecular mechanisms of nitric oxide-induced growth arrest and apoptosis in fetal pulmonary arterial smooth muscle cells. *Nitric Oxide* 2003; 9: 201–210.
37. Van der Feen DE, Bartelds B, de Boer RA, et al. Pulmonary arterial hypertension in congenital heart disease: translational opportunities to study the reversibility of pulmonary vascular disease. *Eur Heart J* 2017; 38: 2034–2041.
38. Vozzi F, Bianchi F, Ahluwalia A, et al. Hydrostatic pressure and shear stress affect endothelin-1 and nitric oxide release by endothelial cells in bioreactors. *Biotechnol J* 2014; 9: 146–154.
39. Toda M, Yamamoto K, Shimizu N, et al. Differential gene responses in endothelial cells exposed to a combination of shear stress and cyclic stretch. *J Biotechnol* 2008; 133: 239–244.
40. Macarthur H, Warner TD, Wood EG, et al. Endothelin-1 release from endothelial cells in culture is elevated both acutely and chronically by short periods of mechanical stretch. *Biochem Biophys Res Commun* 1994; 200: 395–340.
41. Lauth M, Berger MM, Cattaruzza M, et al. Elevated perfusion pressure upregulates endothelin-1 and endothelin B receptor expression in the rabbit carotid artery. *Hypertension* 2000; 35: 648–654.
42. Kuchan MJ and Frangos JA. Shear stress regulates endothelin-1 release via protein kinase C and cGMP in cultured endothelial cells. *Am J Physiol* 1993; 264: H150–H156.
43. Morawietz H, Talanow R, Szibor M, et al. Regulation of the endothelin system by shear stress in human endothelial cells. *J Physiol* 2000; 525: 761–770.
44. Lauth M, Berger MM, Cattaruzza M, et al. Pressure-induced upregulation of preproendothelin-1 and endothelin B receptor expression in rabbit jugular vein in situ: implications for vein graft failure? *Arterioscler Thromb Vasc Biol* 2000; 20: 96–103.
45. Li M, Stenmark KR, Shandas R, et al. Effects of pathological flow on pulmonary artery endothelial production of vasoactive mediators and growth factors. *J Vasc Res* 2009; 46: 561–571.

46. Wedgwood S, Lakshminrusimha S, Schumacker PT, et al. Cyclic stretch stimulates mitochondrial reactive oxygen species and Nox4 signaling in pulmonary artery smooth muscle cells. *Am J Physiol Lung Cell Mol Physiol* 2015; 309: L196–L203.
47. Wang CC, Ying L, Barnes EA, et al. Pulmonary artery smooth muscle cell HIF-1 α regulates endothelin expression via microRNA-543. *Am J Physiol* 2018; 315: L422–L431.
48. Archer SL, Gomberg-Maitland M, Maitland ML, et al. Mitochondrial metabolism, redox signaling, and fusion: a mitochondria-ROS-HIF-1alpha-Kv1.5 O2-sensing pathway at the intersection of pulmonary hypertension and cancer. *Am J Physiol* 2008; 294: H570–H578.
49. Zemskov EA, Lu Q, Ornatowski W, et al. Biomechanical forces and oxidative stress: implications for pulmonary vascular disease. *Antioxid Redox Signal* 2019; 31: 819–842.
50. Belaidi E, Morand J, Gras E, et al. Targeting the ROS-HIF-1-endothelin axis as a therapeutic approach for the treatment of obstructive sleep apnea-related cardiovascular complications. *Pharmacol Ther* 2016; 169: 1–11.
51. Avitabile CM, Vorhies EE and Ivy DD. Drug treatment of pulmonary hypertension in children. *Paediatr Drugs* 2020; 22: 123–147.